Article ID: 1003－6326(2005)05－1021－05

Influence of Cr or Co doping on electrode properties of $V_{2.1}TiNi_{0.5}Hf_{0.05}$ hydrogen storage alloy①

CHEN Li-xin(陈立新), GUO Rui(郭 蕊),
LI Lu(李 露), LEI Yong-quan(雷永泉)
(College of Materials Science and Chemical Engineering, Zhejiang University,
Hangzhou 310027, China)

Abstract: The microstructures and electrode properties of Cr or Co-doped $V_{2.1}TiNi_{0.5}Hf_{0.05}M_{0.113}$ (M = Cr, Co) hydrogen storage alloys were investigated. It is found that all alloys consist of a main phase of V-based solid solution with b. c. c. structure and a secondary phase of C14-type Laves phase with a three-dimensional network structure. After the doping of Cr or Co into $V_{2.1}TiNi_{0.5}Hf_{0.05}$, the abundance and unit cell volume of the main phase decrease, and those of the secondary phase increase. The electrochemical measurements show that the discharge capacities of Cr-doped $V_{2.1}TiNi_{0.5}Hf_{0.05}Cr_{0.113}$ alloy and Co-doped $V_{2.1}TiNi_{0.5}Hf_{0.05}Co_{0.113}$ alloy are less than that of $V_{2.1}TiNi_{0.5}Hf_{0.05}$ alloy, but their cycle stability and high-rate dischargeability are improved markedly. The results show that Cr or Co doping into $V_{2.1}TiNi_{0.5}Hf_{0.05}$ alloy is significantly beneficial for the cycling stability.

Key words: V-based hydrogen storage alloys; Cr doping; Co doping; electrode properties; microstructure
CLC number: TG 139.7 **Document code:** A

1 INTRODUCTION

Vanadium-based solid solution electrode alloys have attracted the attention of scientists since the $V_3TiNi_{0.56}$ alloy with high electrochemical discharge capacity was reported[1]. These alloys characteristically consist of two phases: a vanadium-based solid solution as main phase and a secondary phase, which work as a hydrogen storage phase and a micro-current collector, respectively. However, the poor cycling stability of these alloys in KOH electrolyte keeps them from the industrialization for Ni-MH batteries. The influence of various additive elements to $V_3TiNi_{0.56}$ alloy was investigated for improving the electrode properties, especially the cycling stability[2-7]. The results show that multi-component alloying is an effective method for improving the overall properties of the hydrogen storage electrode alloys[8-12]. In our previous works, $V_{2.1}TiNi_{0.5}Hf_{0.05}$ was found to have a high discharge capacity of 444 mA·h/g and a poor cycling capacity retention of 27.66% after 30 cycles[13]. In this paper, Cr and Co were chosen as the added alloying elements into $V_{2.1}TiNi_{0.5}Hf_{0.05}$ for improving its cycling stability, and the microstructure and electrode properties of $V_{2.1}TiNi_{0.5}Hf_{0.05}M_{0.113}$ (M = Cr, Co) hydrogen storage alloys were investigated systematically.

2 EXPERIMENTAL

The alloy samples were prepared by vacuum induction melting under argon atmosphere and each batch was remelted three times to ensure high homogeneity. The metallographic microstructures were examined by using a scanning electron microscope(SEM). The chemical compositions of the overall alloys and the contents of alloy elements in the KOH electrolyte after charging-discharging cycles were confirmed by using an inductively coupled plasma technique(ICP), and the chemical compositions of micro-area for each phase were determined with an energy dispersive X-ray spectrometer(EDS). The crystal structures and lattice parameters were determined by X-ray powder diffraction(XRD) using Cu K_α radiation.

The samples were pulverized first by hydriding and then crushed mechanically into particles below 50 μm in size after dehydriding. Each test electrode was prepared by mixing alloy powders with copper powders in the mass ratio of 1∶2 and then the mixture was cold-pressed into a pellet. The electrochemical properties of these negative electrodes were measured in a tri-electrode open cell at 298 K with a sintered $Ni(OH)_2$/NiOOH positive counter electrode and a Hg/HgO reference electrode. The negative electrodes were charged at 100 mA/g for 6.5 h and discharged at 25－500 mA/g to

① **Foundation item:** Project(50271064) supported by the National Natural Science Foundation of China; Project(2003AA515021) supported by the Hi-Tech Research and Development Program of China
Received date: 2005－02－08; **Accepted date:** 2005－07－01
Correspondence: CHEN Li-xin, Associate professor, PhD; Tel: +86-571-87951152; E-mail: lxchen@zju.edu.cn

the cutoff potential of – 0.70 V vs Hg/HgO. The electrochemical hydrogen desorption P-C isotherms at 298 K were plotted by using the pulse charge/discharge method at 25 mA/g, and the hydrogen desorption equilibrium pressure(p_{eq}) was calculated from the measured equilibrium electrode potential(E_{eq}) according to the Nernst equation[14]:

$$E_{eq}(\text{V vs Hg/HgO}) = -0.93045 - 0.029547\log(p_{eq})$$

The exchange current density I_o of the alloys was calculated from the slopes of micro-polarization curves, which were determined by scanning the electrode potential at 0.1 mV/s from – 5 mV to 5 mV (vs open circuit potential) with a Solartron SI 1287 potentiostat.

3 RESULTS AND DISCUSSION

3.1 Microstructure

Fig. 1 shows the XRD patterns of $V_{2.1}TiNi_{0.5}Hf_{0.05}M_{0.113}$ (M = Cr, Co) alloys. All of three alloys consist of a main phase of V-based solid solution with b. c. c. structure and a secondary phase of C14-type Laves phase. The calculated unit cell volumes of each phase are shown in Table 1. It can be seen that the unit cell volume of the main phase decreases from 0.02873 nm^3 to 0.02866 nm^3 or 0.02847 nm^3 with adding Cr or Co into the $V_{2.1}TiNi_{0.5}Hf_{0.05}$ alloy, and that of the secondary phase significantly increases from 0.17626 nm^3 to 0.17924 nm^3 or 0.17977 nm^3.

Fig. 2 shows the SEM micrographs of $V_{2.1}TiNi_{0.5}Hf_{0.05}M_{0.113}$ (M = Cr, Co) alloys. It can be seen that the secondary phase all precipitates along the grain boundaries of the main phase in the form of a three-dimensional network. The phase abundance of the main and secondary phases are calculated[15] and shown in Table 1. The amount of the main phase decreases and the amount of the secondary phase increases after adding Cr or Co into the $V_{2.1}TiNi_{0.5}Hf_{0.05}$ alloy.

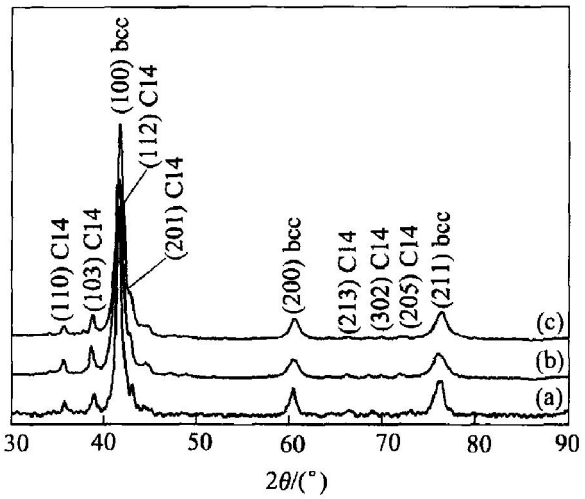

Fig. 1 XRD patterns of alloy samples
(a) —$V_{2.1}TiNi_{0.5}Hf_{0.05}$; (b) —$V_{2.1}TiNi_{0.5}Hf_{0.05}Cr_{0.113}$; (c) —$V_{2.1}TiNi_{0.5}Hf_{0.05}Co_{0.113}$

3.2 Electrochemical characteristics

The activation cycle numbers and maximum discharge capacities of $V_{2.1}TiNi_{0.5}Hf_{0.05}M_{0.113}$ (M = Cr, Co) alloys are shown in Table 2. It can be seen that the activation cycle number increases from 1 to 2 after the doping of Cr or Co. $V_{2.1}TiNi_{0.5}Hf_{0.05}$ has the highest discharge capacity of 444 mA · h/g, much higher than that of $V_{2.1}TiNi_{0.5}Hf_{0.05}Cr_{0.113}$ (392 mA · h/g) and $V_{2.1}TiNi_{0.5}Hf_{0.05}Co_{0.113}$ (386 mA · h/g). The electrochemical P-C desorption isotherms of the alloys are shown in Fig. 3. The results indicate that the plateau pressure rises and the width of pressure plateau reduces after adding Cr or Co into the $V_{2.1}TiNi_{0.5}Hf_{0.05}$ alloy. The decrease of the discharge capacity due to the doping of Cr or Co could be ascribed to the decrease of the phase abundance and the unit cell volumes of the main phase. The later could be mainly responsible for the decrease, because comparing with $V_{2.1}TiNi_{0.5}Hf_{0.05}$, the equilibrium hydrogen pressure of $V_{2.1}TiNi_{0.5}Hf_{0.05}Cr_{0.113}$ or $V_{2.1}TiNi_{0.5}Hf_{0.05}Co_{0.113}$ is almost the same or distinctly high-

Table 1 Micro-structural characteristics of alloy samples

Alloy	Phase	Composition (mole fraction)/%						Phase abundance/%	Unit cell volume/nm^3
		V	Ti	Ni	Hf	Cr	Co		
$V_{2.1}TiNi_{0.5}Hf_{0.05}$	Main phase	75.23	19.44	5.28	0.04	–	–	0.69	0.02873
	Secondary phase	15.98	44.51	36.01	3.50	–	–	0.31	0.17626
$V_{2.1}TiNi_{0.5}Hf_{0.05}Cr_{0.113}$	Main phase	76.67	15.87	3.81	0	3.65	–	0.60	0.02866
	Secondary phase	24.80	40.00	30.80	2.80	1.60	–	0.40	0.17924
$V_{2.1}TiNi_{0.5}Hf_{0.05}Co_{0.113}$	Main phase	76.09	16.84	4.88	0.67	–	1.52	0.58	0.02847
	Secondary phase	25.32	42.19	25.74	2.53	–	4.22	0.42	0.17977

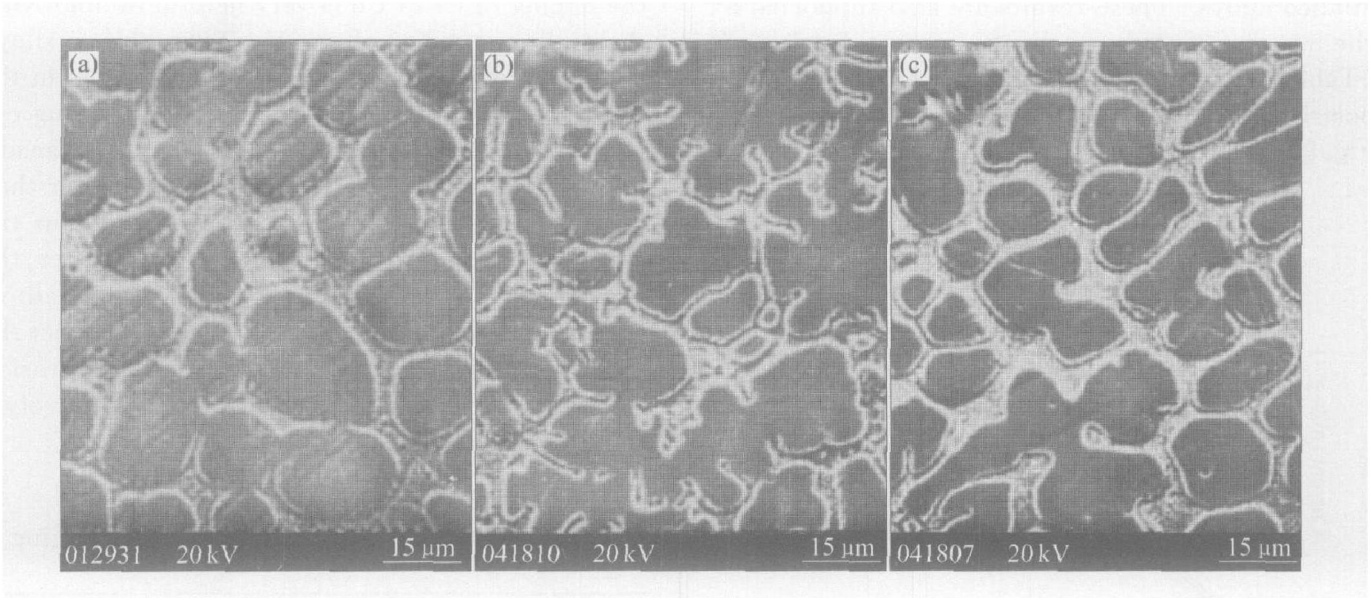

Fig. 2 SEM micrographs of alloy samples
(a) —$V_{2.1}TiNi_{0.5}Hf_{0.05}$; (b) —$V_{2.1}TiNi_{0.5}Hf_{0.05}Cr_{0.113}$; (c) —$V_{2.1}TiNi_{0.5}Hf_{0.05}Co_{0.113}$

Table 2 Electrochemical properties of alloy samples

Alloy	Activation cycle number*	Discharge capacity* / (mA · h · g^{-1})	High-rate dischargeability**, HRD400/%	Exchange current density(I_o) / (mA · g^{-1})	Capacity retention/%	
					After 30 cycles	After 60 cycles
$V_{2.1}TiNi_{0.5}Hf_{0.05}$	1	444	26.50	96.14	27.66	–
$V_{2.1}TiNi_{0.5}Hf_{0.05}Cr_{0.113}$	2	392	58.68	120.5	70.11	38.07
$V_{2.1}TiNi_{0.5}Hf_{0.05}Co_{0.113}$	2	386	47.60	107.8	71.42	50.52

* Alloy electrodes were charged at 100 mA/g and discharged at 25 mA/g.
* * High-rate dischargeability at discharge current density of 400 mA/g.

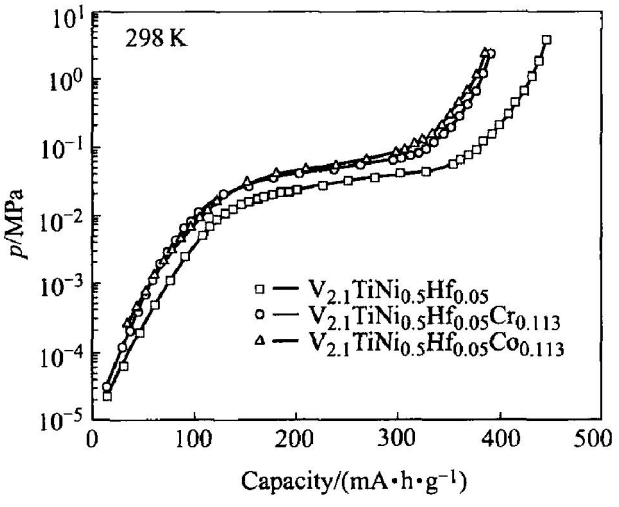

Fig. 3 Electrochemical P-C desorption isotherms of alloy samples

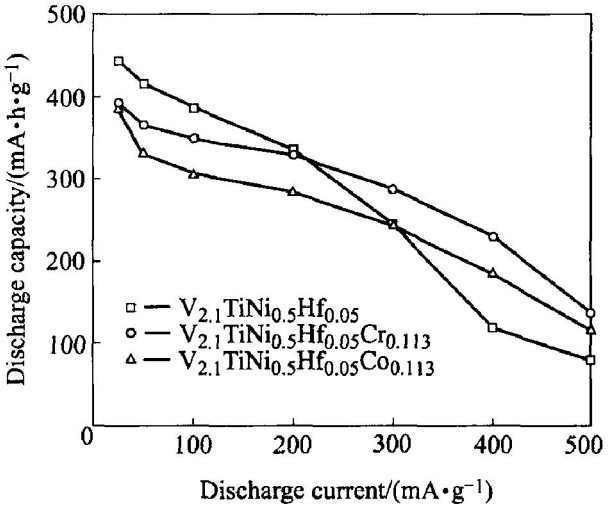

Fig. 4 Relation between discharge capacity and discharge current density for alloy samples

er, respectively, while a smaller cell volume generally leads to a higher equilibrium pressure[16].

The relation between discharge capacity and discharge current density for $V_{2.1}TiNi_{0.5}Hf_{0.05}M_{0.113}$ (M= Cr, Co) alloys is shown in Fig. 4. At larger discharge current densities (400 - 500 mA/g), the discharge capacities of $V_{2.1}TiNi_{0.5}Hf_{0.05}Cr_{0.113}$ and $V_{2.1}TiNi_{0.5}Hf_{0.05}Co_{0.113}$ are much higher than that of $V_{2.1}TiNi_{0.5}Hf_{0.05}$. The high-rate dischargeability (HRD400 = C400/C25 (100%) of these alloys at the discharge current density of 400 mA/g is shown in Table 2. It can be seen that $V_{2.1}TiNi_{0.5}Hf_{0.05}Cr_{0.113}$ has the best high-rate dischargeability (HRD400 of 58.68%) among the

studied alloys. These results are also supported by the magnitude of the exchange current densities I_o (Table 2) calculated from the slopes of the micro-polarization curves of these alloys as shown in Fig. 5.

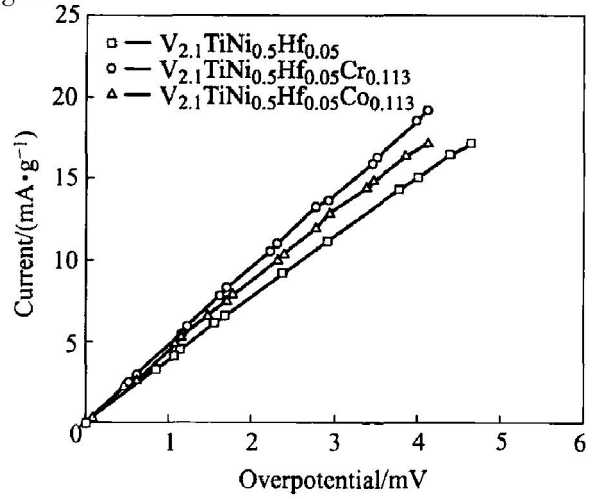

Fig. 5 Micro-polarization curves of alloy electrodes

Fig. 6 shows the cycling capacity degradation curves of the $V_{2.1}TiNi_{0.5}Hf_{0.05}M_{0.113}$ (M= Cr, Co) alloys. All of the alloys were activated within two charging-discharging cycles. The discharge capacity of $V_{2.1}TiNi_{0.5}Hf_{0.05}$ reduces rapidly and its capacity retention after 30 cycles is only 27.66%. However, the degradation of $V_{2.1}TiNi_{0.5}Hf_{0.05}Cr_{0.113}$ or $V_{2.1}TiNi_{0.5}Hf_{0.05}Co_{0.113}$ is slow comparatively. As shown in Table 2, the capacity retention of $V_{2.1}TiNi_{0.5}Hf_{0.05}Cr_{0.113}$ is 70.11% after 30 cycles and 38.07% after 60 cycles, and the capacity retention of $V_{2.1}TiNi_{0.5}Hf_{0.05}Co_{0.113}$ is 71.42% after 30 cycles and 50.52% after 60 cycles, much better than that of $V_{2.1}TiNi_{0.5}Hf_{0.05}$. These indicate that

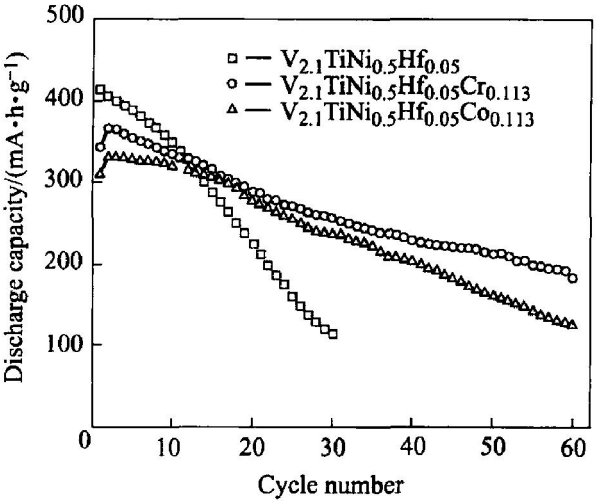

Fig. 6 Cycling capacity degradation curves of alloy samples charged at 100 mA/g and discharged at 50 mA/g

the doping of Cr or Co is very helpful in improving the cycling stability of the $V_{2.1}TiNi_{0.5}Hf_{0.05}$ alloy. Table 3 shows the content of alloy elements in the KOH electrolyte after 30 charging-discharging cycles. It can be seen that the dissolution of vanadium in the alloy into KOH electrolyte is faster than other elements, and the vanadium content in the electrolyte solution decreases markedly after the doping of Cr or Co into the $V_{2.1}TiNi_{0.5}Hf_{0.05}$ alloy. This result indicates that Cr and Co can restrict the dissolution of vanadium and improve the corrosion resistance of this series alloys in KOH electrolyte solution noticeably[17, 18].

Table 3 Content of alloy elements in KOH electrolyte after 30 charging-discharging cycles

Alloy	Content/($\mu g \cdot mL^{-1}$)					
	V	Ti	Ni	Hf	Cr	Co
$V_{2.1}TiNi_{0.5}Hf_{0.05}$	30.3	2.6	5.3	0.9	–	–
$V_{2.1}TiNi_{0.5}Hf_{0.05}Cr_{0.113}$	22.8	2.4	5.1	0.9	0.5	–
$V_{2.1}TiNi_{0.5}Hf_{0.05}Co_{0.113}$	21.9	2.4	5.2	0.8	–	0.4

4 CONCLUSIONS

All $V_{2.1}TiNi_{0.5}Hf_{0.05}M_{0.113}$ (M= Cr, Co) alloys consist of a main phase of V-based solid solution with b. c. c. structure and a secondary phase of C14-type Laves phase with a three-dimensional network structure. After the doping of Cr or Co into $V_{2.1}TiNi_{0.5}Hf_{0.05}$, the abundance and unit cell volume of the main phase decrease, and those of the secondary phase increase. The maximum discharge capacities of the Cr-doped and Co-doped alloys are less than that of the $V_{2.1}TiNi_{0.5}Hf_{0.05}$ alloy. However, the doping of Cr or Co into the $V_{2.1}TiNi_{0.5}$-$Hf_{0.05}$ alloy is significantly beneficial for the cycling stability and high-rate dischargeability.

REFERENCES

[1] Tsukahara M, Takahashi K, Mishima T, et al. Phase structure of V-based solid solutions containing Ti and Ni and their hydrogen absorption-desorption properties [J]. J Alloys and Compounds, 1995, 224(1): 162-167.

[2] Tsukahara M, Takahashi K, Mishima T, et al. Metal hydride electrodes based on solid solution type alloy TiV_3Ni_x ($0 \leqslant x \leqslant 0.75$) [J]. J Alloys and Compounds, 1995, 226(1-2): 203-207.

[3] Tsukahara M, Takahashi K, Mishima T, et al. Influence of various additives in vanadium-based alloys $V_3TiNi_{0.56}$ on secondary phase formation, hydrogen storage properties and electrode properties [J], J Alloys and Compounds, 1996, 245(1-2): 59-65.

[4] Tsukahara M, Takahashi K, Isomura A, et al. Improvement of the cycle stability of vanadium-based

alloy for nickel-metal hydride (Ni-MH) battery [J]. J Alloys and Compounds, 1999, 287(1-2): 215-220.
[5] YU X B, WU Z, XIA B J, et al. A Ti-V-based bcc phase alloy for use as metal hydride electrode with high discharge capacity [J]. J of Chemical Physics, 2004, 121(2): 987-990.
[6] YU X B, WU Z, XIA B J, et al. Electrochemical performance of ball-milled Ti-V-based electrode alloy [J]. Int J Hydrogen Energy, 2005, 30(3): 273-277.
[7] CHEN Li-xin, DAI Fa-bang, LIU Jian, et al. Influence of ball-milling with Cu powder on the electrochemical properties of V-based solid solution type hydrogen storage alloys [J]. The Chinese Journal of Nonferrous Metals, 2005, 15(4): 661-666. (in Chinese)
[8] ZHANG Q A, LEI Y Q, YANG X G, et al. Influence of Mn on phase structures and electrochemical properties of $V_3TiNi_{0.56}Hf_{0.24}$ alloy [J]. Int J Hydrogen Energy, 2000, 25(7): 657-661.
[9] ZHANG Q A, LEI Y Q, YANG X G, et al. Phase structures and electrochemical properties of $V_3TiNi_{0.56}Hf_{0.24}Co_x$ alloy [J]. J Alloys and Compounds, 2000, 296(1-2): 87-91.
[10] ZHANG Q A, LEI Y Q, YANG X G, et al. Phase structures and electrochemical properties of Cr-added $V_3TiNi_{0.56}Hf_{0.24}Mn_{0.15}$ alloys [J]. Int J Hydrogen Energy, 2000, 25(10): 977-981.
[11] ZHANG Y, LI S Q, CHEN L X, et al. Corrosion mechanism of mechanically alloyed $Mg_{50}Ni_{50}$ and $Mg_{45}Cu_5Ni_{50}$ alloys [J]. Trans Nonferrous Metals Soc China, 2002, 12(2): 238-241.
[12] CHEN X L, LEI Y Q, LIAO B, et al. Effects of annealing treatment on microstructure and electrochemical performances of Co-free $MlNi_{4.0}Al_{0.3}Si_{0.1}Fe_{0.6}$ hydrogen storage alloy [J]. The Chinese Journal of Nonferrous Metals, 2004, 14(11): 1862-1868. (in Chinese)
[13] GUO R, CHEN L X, LEI Y Q, et al. The effect of Hf content on the phase structures and electrochemical properties of $V_{2.1}TiNi_{0.5}Hf_x$ (x= 0-0.25) hydrogen storage alloys [J]. J Alloys and Compounds, 2003, 352(1-2): 270-274.
[14] Balej J. Determination of the oxygen and hydrogen overvoltage in concentrated alkali hydroxide solutions [J]. Int J Hydrogen Energy, 1985, 10(6): 365-374.
[15] Tsukahara M, Takahashi K, Mishima T, et al. V-based solid solution alloys with Laves phase network: hydrogen absorption properties and microstructure [J]. J Alloys and Compounds, 1996, 236(1-2): 151-155.
[16] Reilly J J, Adzic G D, Johnson J R, et al. The correlation between composition and electrochemical properties of metal hydride electrodes [J]. J Alloys and Compounds, 1999, 293-295: 569-582.
[17] Ovshinsky S R, Fetcenko M A, Ross J. A nickel metal hydride battery for electric vehicles [J]. Science, 1993, 260: 176-181.
[18] Tsukahara M, Takahashi K, Mishima T, et al. Vanadium-based solid solution alloys with three-dimensional network structure for high capacity metal hydride electrodes [J]. J Alloys and Compounds, 1997, 253-254: 583-586.

(Edited by LI Xiang-qun)